Progress In Electromagnetics Research, Vol. 126, 255–268, 2012

MODIFIED HILBERT-HUANG TRANSFORM AND ITS APPLICATION TO MEASURED MICRO DOPPLER SIGNATURES FROM REALISTIC JET ENGINE MODELS

J. H. Park*, H. Lim, and N. H. Myung

Department of Electrical Engineering, KAIST, 335 Gwahangno, Yuseong-Gu, Daejeon, 305-701, Rep. of Korea

Abstract—Joint time-frequency analysis (JTFA) is applied to micro Doppler signatures generated by jet engine modulation (JEM) effect using a modified Hilbert-Huang transform (HHT). The modified HHT is developed to improve the JTFA results of measured JEM signals. Wavelet decomposition (WD) with Meyer wavelet function is considered as a supplementary process of the HHT. The modified HHT examines a signature obtained from simulation of a jet engine CAD model, and is then applied to the signatures obtained from measurement of two realistic jet engine models. The modified HHT gives more improved JTFA results of the measured JEM signals than those from the simple short-time Fourier transform — (STFT) based analysis. The modified HHT-based JTFA approach is expected to be significantly useful for enabling high-quality radar target recognition in a real environment by complementing other traditional analyses.

1. INTRODUCTION

Jet engine modulation (JEM), one of the most representative radar target recognition methods, is a micro-Doppler effect by radar signals back-scattered from the rotating blades of the jet or aircraft engine compressor. Although multiple time- or frequency-only techniques for the JEM and the JEM field analyses have been studied in recent years [1, 2], joint time-frequency analysis (JTFA) of the JEM signal was not reported until H. Lim presented [3]. In [3], a short-time Fourier transform (STFT) was used for the micro Doppler signatures from

Received 6 January 2012, Accepted 12 March 2012, Scheduled 17 March 2012

* Corresponding author: Ji Hoon Park (dydynoel@kaist.ac.kr).

realistic engine models and extensive studies have been carried out. The JTFA is generally known to provide more intuitive information on the signal characteristics than other conventional time- or frequency-only analyses [4–6]. For a measured JEM signal, however, the JTFA using the STFT was not accurate because of the environmental noise and the inter-modulation effect by the blades in other engine stages. This limitation makes JTFA of the JEM signal unsuitable for radar target recognition in a real environment.

As an extension of JTFA of the measured JEM signals obtained in [3, 7], a recently developed Hilbert-Huang transform (HHT) [8] has been considered with a concentration on the first harmonic generated by the rotation of the first stage blades. Since the HHT was first proposed, it has been used in various fields that deal with non-stationary signals because of its high-resolution characteristic [9–14]. According to the works related to the JTFA using the HHT, the obtained instantaneous Doppler frequency indicated accurate time-dependent characteristics of the Doppler signatures. However, as shortcomings of the HHT were also found, a variety of supplementary processes have been investigated [13, 14].

For the JTFA of the JEM signals, a modified HHT with a supplementary process of the original HHT was developed to improve JTFA results from measured JEM signals. Wavelet decomposition (WD) with Meyer wavelet function was considered as a supplementary process of the HHT. The modified HHT examines a JEM signal simulated from a shooting and bouncing rays (SBR) algorithm- [15, 16] based commercial software package, the virtual aircraft framework (VIRAF). Then it is applied to the JEM signals measured from two experimentally designed jet engine models. With respect to the measured JEM signals, the modified HHT shows that the extracted instantaneous Doppler frequency provides improved estimation results of the number of blades compared with the STFT. Furthermore, the STFT combination with the modified HHT can estimate the blade length with some acceptable error. The modified HHT-based JTFA approach is expected to be significantly useful for high-quality radar target recognition in a real environment by complementing other traditional analyses.

This paper describes the extended JTFA work of the measured JEM micro Doppler signatures from experimentally designed jet engine models using the modified HHT. In Section 2, the theoretical background of the HHT is presented. In Section 3, the modified HHT and its application example are presented. In Section 4, the analysis results of the JEM signals from the measurement are presented. In Section 5, the summary and conclusion are presented.

2. THEORETICAL BACKGROUND OF THE HHT

The HHT was proposed by N. E. Huang for analyzing non-stationary signals originating from non-linear processes. It presents a fundamentally new approach to the JTFA in contrast to the existing time-frequency transforms that generally use integral convolution calculation based on the Fourier transform. The HHT is composed of two steps — empirical mode decomposition (EMD) and Hilbert spectral analysis (HSA).

2.1. Empirical Mode Decomposition (EMD)

EMD is a new type of decomposition algorithm. It decomposes a target signal into a finite number of intrinsic mode functions (IMFs) on the assumption that any data set consists of different, simple and intrinsic modes of oscillation. Each extracted IMF is determined by the nature of the signal and is expected to have a narrow-band component. In addition, the oscillatory mode of the noise component can be separated from that of the micro Doppler signature. Therefore, the EMD is appropriate for the analysis of a signal corrupted by noise components in a real environment. The basic step of the EMD is a sifting process during which the scales of the signal are extracted. An arbitrarily given signal, $x(t)$ can be reconstructed by a simple summation of all the IMFs and the final residue expressed by

$$x(t) = \sum_{i=1}^{n} c_i + r_n, \tag{1}$$

where c_i is the ith component of the IMFs and r_n is the monotonic final residue.

2.2. Hilbert Spectral Analysis (HSA)

Prior to the development of the HHT, the definition of an instantaneous frequency has been controversial for the conventional time-frequency transforms such as the STFT whose formula is expressed by

$$\mathrm{STFT}(t, f) = \int x(t')w(t' - t)e^{-j2\pi ft'}dt', \tag{2}$$

where $x(t)$ is the signal to be transformed, and $w(t)$ is a short-time window function. From (2), the validity of the instantaneous frequency would be guaranteed if the signal were momentarily stationary within the window. The instantaneous frequency in the STFT, however, is a mean frequency over the window. Thus, the STFT calculation

involving the short-time window function always has uncertainty in the form of the frequency spread or frequency blurring. Furthermore, the STFT induces a resolution limitation because the desired time-dependent characteristics of the instantaneous frequency can be shown by a specific short-time window length [3]. In the Hilbert spectral analysis, the definition of the instantaneous frequency becomes clear by the IMFs since they denote the respective intrinsic oscillatory modes. When an arbitrarily given signal $x(t)$ and its Hilbert transform $y(t)$ combine to form an analytic signal $z(t)$, the instantaneous amplitude and the instantaneous phase can be obtained. If the signal $x(t)$ has a narrow-band component as an IMF does, the instantaneous frequency can be defined as

$$\omega(t) = \frac{d\Phi(t)}{dt}, \tag{3}$$

where $\phi(t)$ is the instantaneous phase. The Hilbert spectrum then can be obtained from each IMF in the 3D time-frequency-amplitude plot. It shows the time-dependent characteristic of each intrinsic oscillatory mode included in the target signal.

3. MODIFIED HHT AND ITS APPLICATION EXAMPLE

3.1. Modified HHT

Although the HHT appeared to be a promising tool for analyzing non-stationary signals, its several deficiencies were found and discussed. In essence, the shortcomings of the HHT originate from the EMD. The purpose of the EMD is to decompose the signal into a finite number of intrinsic oscillatory modes rather than into a series of narrow-band components. Consequently, the Hilbert spectrum of each IMF occasionally fails to reveal the instantaneous frequency when the extracted IMF covers a wide frequency range. This failure can lead to misinterpretation of the signal characteristics. As a supplementary process for the EMD, a variety of supplementary methods have been investigated [13, 14]. In order to analyze a JEM signal in the time-frequency domain, a modified HHT with wavelet decomposition (WD) has been developed. The operation procedures of the modified HHT for a JEM signal are summarized in the flowchart in Figure 1.

The parametric model of the JEM developed by Bell [1] describes the JEM spectrum as a periodically generated multi-harmonic spectrum. In a real environment, the first harmonic is relatively easier to be observed than other harmonics. The JEM is dominantly produced by the rotation of the first stage blades which mostly scatter the incident radar signature. Therefore, the JEM micro Doppler

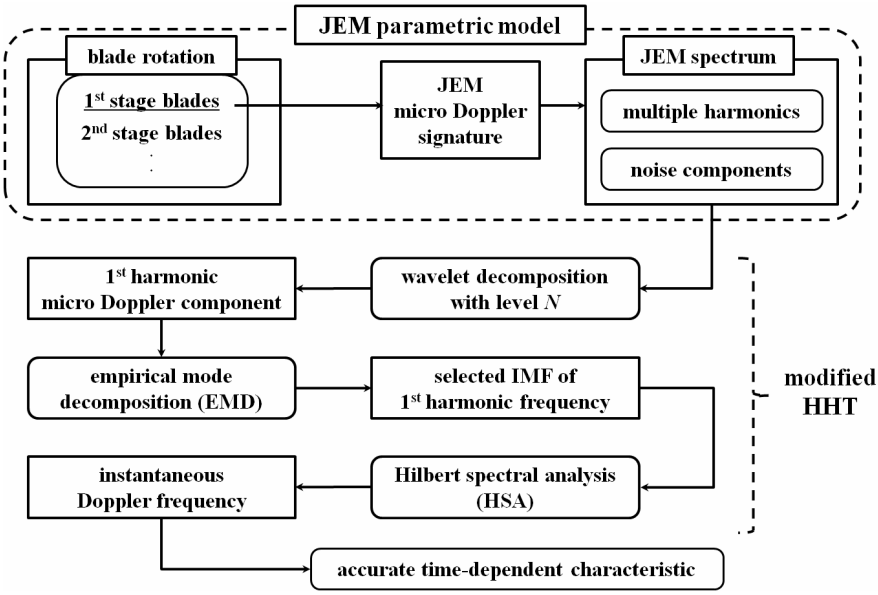

Figure 1. The operation procedures of modified HHT for JTFA of a JEM signal.

characteristic generated by the first stage blades can be extracted using the first harmonic of the JEM spectrum. The WD can be a good supplementary preprocessor of the HHT since it is suitable for the extraction of the first harmonic and requires less computation than other supplementary methods. During the operation of WD [17, 18], the original JEM signal is divided into an approximation component (A1) and a detail component (D1) through a low-band filter (LF) and a high-band filter (HF), respectively. Then the A1 is further split into AA2 and AD2 at the decomposition level 2. The process is continued until the decomposition level reaches the adaptively determined value N expressed by

$$N < \left\lfloor \log\left(\frac{f_s/2}{f_1}\right) / \log 2 \right\rfloor, \tag{4}$$

where f_1 is the first harmonic frequency, $f_s/2$ is the sampling frequency or pulse repetition frequency (PRF) of the radar signature with a positive frequency range, and "$\lfloor\,\rfloor$" is the floor operator that outputs the largest integer not greater than the input value. The first harmonic frequency can be obtained from a simple and traditional spectral analysis. For the mother wavelet function, a discrete Meyer wavelet

function was adopted because it is known to be appropriate for harmonic analysis [19, 20]. With the WD prior to the EMD, there can be less possibility that each extracted IMF has multiple frequency components because the WD limits the frequency band larger than the first harmonic frequency. After the selection of an IMF corresponding to the first harmonic frequency, the instantaneous Doppler frequency of the IMF containing the micro Doppler component can be obtained. When the modified HHT is used, the WD allows the selected IMF to characterize the micro Doppler signature correctly. Furthermore, the noise component that caused the improper results of the STFT can be discriminated and separated by the EMD. Therefore, an accurate time-dependent characteristic of the JEM micro Doppler signature is expected to be revealed from the instantaneous Doppler frequency plotted in the Hilbert spectrum.

3.2. An Application Example

To give an Application example, the modified HHT was applied to a JEM signal obtained from a SBR-based VIRAF simulation of a realistic jet engine CAD model. The detailed simulation procedure is described in [3]. Summarized information on the jet engine CAD model and the simulation parameters are given in Table 1.

The first harmonic frequency obtained from a spectral analysis is 4 kHz. Since the PRF is 80 kHz, WD with a level 3 is applied to the signal as described in (4). The spectrum of the signal after the WD contains only the first harmonic and the zero Doppler component generated by the engine structure itself. When the EMD is applied to the decomposed signal subsequently, an IMF corresponding to the first harmonic frequency can be extracted. Using the Hilbert transform, the Hilbert spectrum for the selected IMF is obtained and provides

Table 1. The information on the jet engine CAD model and VIRAF simulation parameters.

complete CAD model	stage number	1	2	3	4
	number of blades	40	88	96	108
	radar frequency	10 GHz			
	PRF	80 kHz			
	number of bursts	1600			
	rotation speed	6000 RPM			
	incident angle	10 deg			

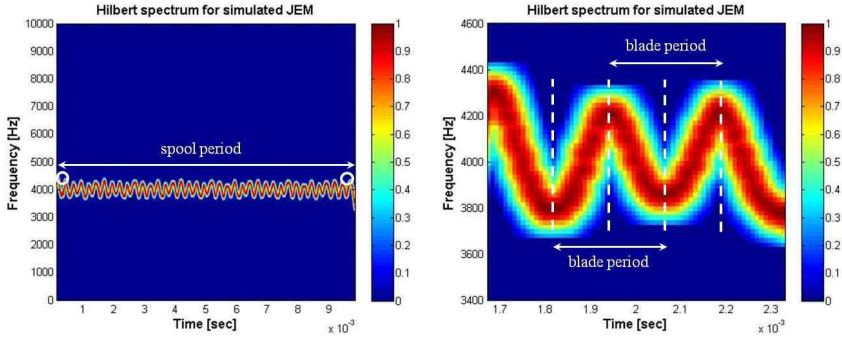

Figure 2. HHT result of the simulated JEM signal. (a) The Hilbert spectrum of the instantaneous Doppler frequency, (b) expanded Hilbert spectrum related to (a).

the exact time-dependent characteristic of the instantaneous Doppler frequency as shown in Figure 2. The spool period for one revolution obtained from autocorrelation analysis [1, 3] is 0.01 sec in accordance with the rotation speed given in Table 1. Centered at the first harmonic frequency, the instantaneous Doppler frequency distinctly shows the sinusoidal waveform of the JEM micro Doppler signature, with the repetition of increase and decrease by the blade period. The blade period indicates the period when a blade rotates from the original position to the adjacent position. From the expanded Hilbert spectrum shown in Figure 2(b), the blade period is calculated as 0.251 msec. Being in good agreement with the real number of the blades, the calculated number of blades is 40 with an error of less than 0.4%. This application example confirms that the desired time-dependent characteristic of the JEM micro Doppler signature can be extracted using the modified HHT. The instantaneous Doppler frequency was obtained without the time-frequency resolution limitation induced by the STFT window function.

For the simulated JEM signal, the environmental noise and the inter-modulation effect by the second and third stage blades were regarded as being negligible. Thus, the JEM harmonics produced by the rotation of first stage blades could be clearly observed from the JEM spectrum. For the measured JEM signal, however, it is difficult for the JEM harmonics to be discriminated definitely by noise components. In the next section, the modified HHT is applied to the measured JEM signals from two experimentally designed engine models.

4. ANALYSIS RESULTS OF MEASURED JEM SIGNALS

Two realistic jet engine models were designed for acquisition and measurement of JEM signals [3, 7]. Complete figures of the overall engine structure and the rotating parts of the respective engine model are shown in Figure 3. The dimensions and the number of blades in each stage are given in Table 2. In Table 2, D and L denote the overall diameter and length, respectively, and a, b and c denote the

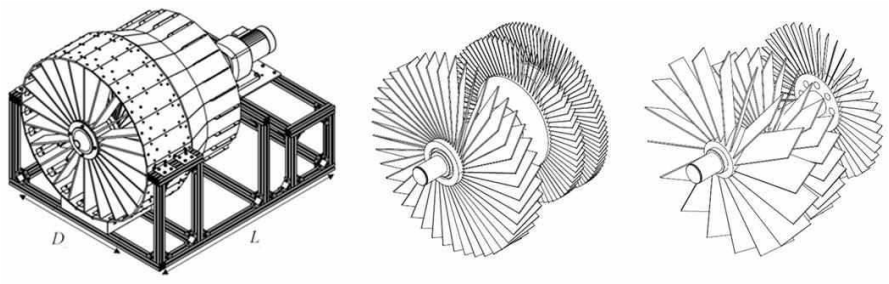

Figure 3. Experimentally designed jet engine models. (a) Isometric view of the overall engine structure, (b) rotating part of engine model A, (c) rotating part of engine model B.

Table 2. Dimensions and the number of blades in each stage of the designed engine models.

model	dimensions [cm]					number of blades		
	D	L	a	b	c	1	2	3
model A	86.6	120	37.7	27.5	27.5	42	73	97
model B	86.6	120	38.5	32.5	30	17	29	41

Table 3. Radar system and jet engine model parameters.

radar frequency	10 GHz
PRF	1.8 kHz
polarization	HH
number of bursts	3600
rotation speed	model A: 60.1 RPM
	model B: 180.3 RPM
incident angle	10 deg

length of the first, second and third stage blades, respectively. The measurement of the JEM signals from the designed jet engine models was performed using vehicle-mounted mobile radar, the ADD vehicle-based RCS instrumentation system (AVRIS) described in [7]. The radar system and the jet engine parameters are given in Table 3.

As shown in Figure 4, the instantaneous Doppler frequency is observed in the Hilbert spectrum of the designed engine model A. The instantaneous Doppler frequency shows a slightly deviated sinusoidal waveform compared with the result shown in Figure 2. This is due to noise components not completely separated from the micro Doppler signature. Concentrating on the segments with good maintenance of

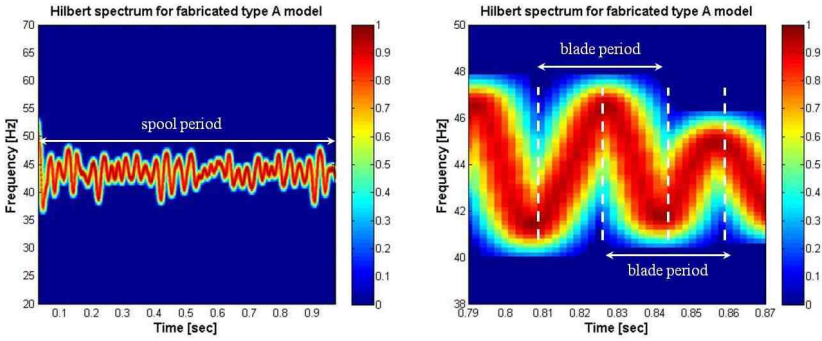

(a) (b)

Figure 4. (a) Hilbert spectrum of the measured JEM signal of designed model A, (b) expanded Hilbert spectrum related to (a).

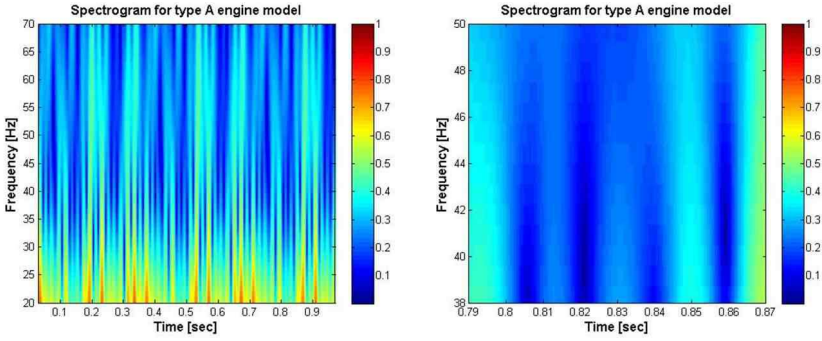

(a) (b)

Figure 5. (a) STFT spectrogram of the measured JEM signal of designed model A, (b) expanded STFT spectrogram related to (a).

the sinusoidal form indicating relatively slight noise corruption, the blade period can be obtained from the Hilbert spectrum. The number of blades is estimated using the spool period and the average observed blade period. To give more insight into the advantage of the modified HHT, the STFT spectrogram of the same signal near the first harmonic is shown in Figure 5 for the comparison between two time-frequency transforms. The Hamming window with the length of 64 was used for the window function. As observed in Figure 5, the spectrogram shows such an irregular and obscure result that the signal characteristics cannot be identified definitely by the noise effect. The micro Doppler component is hard to be recognized near the first harmonic frequency. Furthermore, a time-frequency resolution limitation is also induced by the window function involved in the STFT.

For the designed engine model B, its rotation speed is three times as fast as that of the designed model A. The first harmonic frequency linearly increases as the rotation speed increases [4]. As shown in Figure 6, the instantaneous Doppler frequency is observed in the Hilbert spectrum of the designed engine model B. Although its lower side gives a longer blade period than the theoretical blade period with the error term α, the instantaneous Doppler frequency generally shows a sinusoidal waveform. The error term is regarded as being induced by the selected IMF containing extrinsic frequency components lower than the intrinsic oscillation frequency of the JEM micro Doppler signature. From the Hilbert spectrums of the JEM signals generated by two designed engine models, it has been shown that the modified HHT can estimate the number of blades more accurately than the simple STFT.

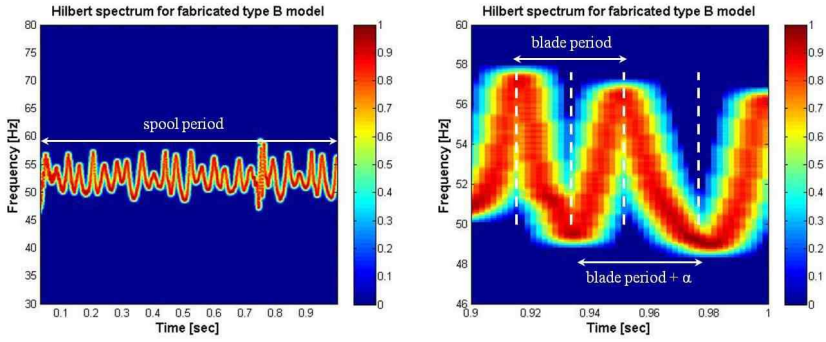

Figure 6. (a) Hilbert spectrum of the measured JEM signal of designed model B, (b) expanded Hilbert spectrum related to (a).

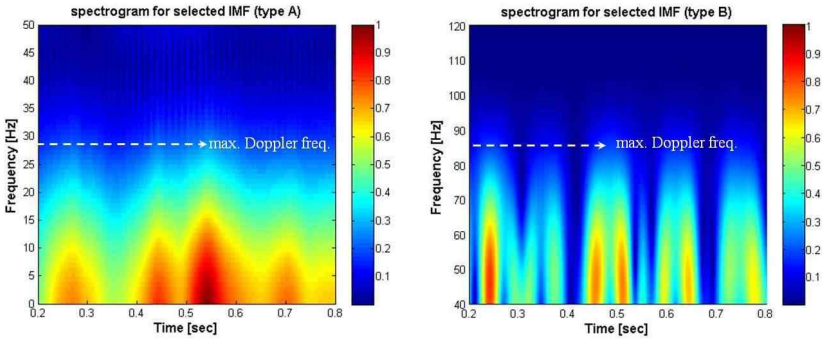

(a) (b)

Figure 7. STFT spectrograms of the selected IMFs. (a) From designed engine model A, (b) from designed engine model B.

Since the instantaneous Doppler frequency just shows the time-dependent characteristic of the JEM micro Doppler signature, it is difficult to estimate the dimension of the blade, namely, the length of the first stage blade. The STFT can be used to obtain the length of the blade from the micro Doppler component because it gives the maximum Doppler frequency range. From the frequency spread in the STFT spectrogram, the outer components that contour the spectrogram indicate the maximum Doppler frequency. As illustrated in Figure 7, the maximum Doppler frequency is determined as the frequency value at the border of the spectrogram whose amplitude is usually 40% of the maximum amplitude. The relation between the maximum Doppler shift frequency and the length of a blade [3] is defined by (5):

$$f_{d,\max} = \frac{2\omega L \sin\theta}{\lambda} + C \tag{5}$$

where $f_{d,\max}$ is the maximum Doppler shift frequency, ω is the angular speed, L is the length of the blade, θ is the incident angle and C is a constant considering the cavity effect of the jet engine structure. By applying the STFT with the Hamming window of length 64 to the selected IMF, the length of the blade can be estimated with some error induced by the residual noise components and the engine cavity effect. In contrast to the spectrogram of the original JEM signal in Figure 5, the spectrograms of the selected IMFs provide more recognizable maximum Doppler shift frequency information because the noise components were separated by the modified HHT. The estimated result of each designed jet engine model is summarized in Table 4.

Table 4. Estimated results: The estimated number of blades of model B becomes 15.01 when the lower side of the instantaneous Doppler frequency is included in the blade period calculation.

designed	number of first stage blades			blade length [cm]		
engine model	real	estimated	error [%]	real	estimated	error [%]
A	42	42.75	1.62	37.7	35.7	5.19
B	17	16.47	3.12	38.5	38.0	1.20

Although the results of the modified HHT give more accurate information than the results of the STFT, some limitations still exist. When the blade period is calculated, there still remain the noise components not completely separated by the EMD. Consequently, the calculated number of blades can be slightly different from the real number by the distorted parts of the instantaneous Doppler frequency. In order to estimate the blade length, a specified window length 64 has to be selected. Further works need to be concentrated on a more complete separation of noise components and more accurate estimation of blade length with a generalized method.

5. CONCLUSION

JTFA of the measured JEM signal was carried out using the modified HHT. Starting from the JEM parametric model, the WD with Meyer wavelet function was adopted as a preprocessor of the HHT. The application of the modified HHT provided the more accurate estimation results of the number of blades than the simple STFT application. Furthermore, the additional STFT application to the selected IMF could estimate the blade length more precisely. The modified HHT-based JTFA approach described in this paper is expected to allow advanced and high-quality radar target recognition in a real environment.

ACKNOWLEDGMENT

This research was supported by the Agency for Defense Development (ADD), Rep. of Korea.

REFERENCES

1. Bell, M. R. and R. A. Grubbs, "JEM modeling and measurement for radar target identification," *IEEE Trans. Aerospace and Electronic Systems*, Vol. 29, No. 1, 73–87, 1993.
2. Lim, H. and N.-H. Myung, "A novel hybrid AIPO-MoM technique for jet engine modulation analysis," *Progress In Electromagnetics Research*, Vol. 104, 85–97, 2010.
3. Park, J. H., J. H. Yoo, C. H. Kim, K. I. Kwon, and N. H. Myung, "Joint time-frequency analysis of radar micro-Doppler signatures from aircraft engine models," *Journal of Electromagnetic Waves and Applications*, Vol. 25, Nos. 8–9, 1069–1080, 2011.
4. Chen, V. C. and H. Ling, *Time-Frequency Transforms for Radar Imaging and Signal Analysis*, Chapter 8, Artech House, Norwood, MA, 2002.
5. Han, S.-K., H.-T. Kim, S.-H. Park, and K.-T. Kim, "Efficient radar target recognition using a combination of range profile and time-frequency analysis," *Progress In Electromagnetics Research*, Vol. 108, 131–140, 2010.
6. Guo, K. Y., Q. Li, and X. Q. Sheng, "A precise recognition method of missile warhead and decoy in multi-target scene," *Journal of Electromagnetic Waves and Applications*, Vol. 24, Nos. 5–6, 641–652, 2010.
7. Lim, H., J. H. Yoo, C. H. Kim, K. I. Kwon, and N. H. Myung, "Radar cross section measurement of a realistic jet engine structure with rotating parts," *Journal of Electromagnetic Waves and Applications*, Vol. 25, No. 7, 999–1008, 2011.
8. Huang, N. E., Z. Shen, S. R. Long, M. C. Wu, H. H. Shih, Q. Zheng, N. C. Yen, C. C. Tung, and H. H. Liu, "The empirical mode decomposition and the Hilbert spectrum for nonlinear and non-stationary time series analysis," *Proc. R. Soc. A*, Vol. 454, No. 1971, 679–699, 1998.
9. Liu, Z., L. Liu, and B. Barrowes, "The application of the Hilbert-Huang transform in through-wall life detection with UWB impulse radar," *PIERS Online*, Vol. 6, No. 7, 695–699, 2010.
10. Yan, R. and R. X. Gao, "Hilbert-Huang transform-based vibration signal analysis for machine health monitoring," *IEEE Trans. Instrumentation and Measurement*, Vol. 55, No. 6, 1327–1334, 2006.
11. Cai, C., W. Liu, J. S. Fu, and Y. Lu, "Radar micro-Doppler signature analysis with HHT," *IEEE Trans. Aerospace and Electronic Systems*, Vol. 46, No. 2, 929–938, 2010.

12. Narayanan, R. M., M. C. Shastry, P.-H. Chen, and M. Levi, "Through-the-wall detection of stationary human targets using Doppler radar," *Progress In Electromagnetics Research B*, Vol. 20, 147–166, 2010.
13. Yang, W., "Interpretation of mechanical signals using an improved Hilbert-Huang transform," *Mechanical System and Signal Processing*, No. 22, 1061–1071, 2008.
14. Peng, Z., P. Tse, and F. Chu, "An improved Hilbert-Huang transform and its application in vibration signal analysis," *Journal of Sound and Vibration*, No. 286, 187–205, 2005.
15. Gao, P. C., Y. B. Tao, and H. Lin, "Fast RCS prediction using multiresolution shooting and bouncing ray method on the GPU," *Progress In Electromagnetics Research*, Vol. 107, 187–202, 2010.
16. Buddendick, H. and T. F. Eibert, "Bistatic image formation from shooting and bouncing rays simulated current distributions," *Progress In Electromagnetics Research*, Vol. 119, 1–18, 2011.
17. Chen, G. P. and Z. Q. Zhao, "Ultrasound tomography-guide TRM technique for breast tumor detecting in MITAT system," *Journal of Electromagnetic Waves and Applications*, Vol. 24, Nos. 11–12, 1459–1471, 2010.
18. Ramesh, R., M. Madheswara, and K. Kannan, "Numerical simulation of nanoscale FinFET photodetector for optimal detection of biological signals using interpolating wavelets," *Progress In Electromagnetics Research B*, Vol. 31, 239–260, 2011.
19. Hatamzadeh-Varmazyar, S., M. Naser-Moghadasi, E. Babolian, and Z. Masouri, "Calculating the radar cross section of the resistive targets using the Haar wavelets," *Progress In Electromagnetics Research*, Vol. 86, 55–80, 2008.
20. Zhang, M., Y. W. Zhao, H. Chen, and W.-Q. Jiang, "SAR imaging simulation for composite model of ship on dynamic ocean scene," *Progress In Electromagnetics Research*, Vol. 113, 395–412, 2011.